J Geod (2014) 88:1061–1079
DOI 10.1007/s00190-014-0743-7

ORIGINAL ARTICLE

On the Mátern covariance family: a proposal for modeling temporal correlations based on turbulence theory

Gaël Kermarrec · Steffen Schön

Received: 7 January 2014 / Accepted: 10 June 2014 / Published online: 2 July 2014

Abstract Current variance models for GPS carrier phases that take correlation due to tropospheric turbulence into account are mathematically difficult to handle due to numerical integrations. In this paper, a new model for temporal correlations of GPS phase measurements based on turbulence theory is proposed that overcomes this issue. Moreover, we show that the obtained model belongs to the Mátern covariance family with a smoothness of 5/6 as well as a correlation time between 125–175 s. For this purpose, the concept of separation distance between two lines-of-sight introduced by Schön and Brunner (J Geod 1:47–57, 2008a) is extended. The approximations made are highlighted as well as the turbulence parameters that should be taken into account in our modeling. Subsequently, fully populated covariance matrices are easily computed and integrated in the weighted least-squares model. Batch solutions of coordinates are derived to show the impact of fully populated covariance matrices on the least-squares adjustments as well as to study the influence of the smoothness and correlation time. Results for a specially designed network with weak multipath are presented by means of the coordinate scatter and the a posteriori coordinate precision. It is shown that the known overestimation of the coordinate precision is significantly reduced and the coordinate scatter slightly improved in the sub-millimeter level compared to solutions obtained with diagonal, elevation-dependent covariance matrices. Even if the variations are small, turbulence-based values for the smoothness and correlation time yield best results for the coordinate scatter.

Keywords GPS · Physical correlations · Temporal correlations · Turbulence theory · Mátern covariance family

G. Kermarrec (✉) · S. Schön
Institut für Erdmessung (IfE), Leibniz Universität Hannover,
Schneiderberg 50, 30167 Hannover, Germany
e-mail: gael.kermarrec@web.de

S. Schön
e-mail: schoen@ife.uni-hannover.de

1 Introduction

The use of diagonal covariance matrices in which temporal correlations between GPS phase measurements are ignored leads to unreliable positioning results and an overestimation of the precision (El-Rabbany 1994; Wang et al. 2002; Satirapod et al. 2003). Being mainly computed with elevation-dependent models (Euler and Goad 1991), C/N0 models (Hartinger and Brunner 1999; Brunner et al. 1999; Wieser and Brunner 2000), or SNR models (Luo et al. 2011), diagonal covariance matrices are however easy to handle in weighted least-squares models since no computational issue due to matrix inversions occurs (Howind et al. 1999; Beutler et al. 1987). Leading to fully populated variance–covariance matrices (VCM), temporal correlations can depend on receiver type, occur between channels and observation types (Borre and Tiberius 2000) or come from multipath (Radovanovic 2001). However, the main temporal correlations are known to come from the GNSS signal propagation through the atmosphere, considered as a random medium.

Up to now, few propositions have been done to specify time-dependent correlations. El-Rabbany (1994) proposed an empirical modeling based on the study of autocorrelation functions of phase residuals which leads to a simple exponential function with an empirically determined correlation time. Howind et al. (1999) used the results of El-Rabbany to build covariance matrices. They principally showed that the coor-

dinate estimates are not much improved; nevertheless, the a posteriori accuracy of the least-squares solution is much more realistic. Wang et al. (2002) and Satirapod et al. (2003) used a recursive whitening procedure based on residuals. They highlighted that the determination of ambiguities was strongly improved. In the last few years, some authors have also made used of ARMA processes at the least-squares residuals' level to study temporal correlations of GPS measurements (Luo et al. 2012; Wang et al. 2002).

Based on Kolmogorov turbulence theory and the concept of eddies, Schön and Brunner (2008a) developed the SIGMA-C model. This model, as the Treuhaft and Lanyi (1987) one, is involving a double integration, making its concrete use time consuming. Thus, until yet, there is a lack of a simple, physically derived and easy to handle model for temporal GPS phase correlations.

Thanks to the equations of electromagnetic propagation and geometrical approximations as well as the Kolmogorov turbulence theory, we develop a new covariance model, based on the flexible Mátern covariance family. Using the results of Schön and Brunner (2008a), it is possible to estimate covariances between phase observations for all relevant cases, i.e.

- a given satellite observed at one station with itself,
- one satellite at one station with another one at the same station,
- one satellite at a given station with another one at another station.

Thanks to the specially designed "Seewinkel Network" (Schön and Brunner 2008b), first promising results, both for the quadratic deviation of the computed batch coordinates as well as for the a posteriori variance of the unknowns validate the feasibility and the utility of taking temporal correlations into account with the Mátern covariance family.

The paper is organized as follow: in a first part, a new way to model GPS phase temporal correlations based on models using turbulence (Schön and Brunner 2008a) will be presented. The second part is devoted to the comparison with other models as well as the study of the model parameter dependencies. In a last part, a concrete case based on the Seewinkel Network, designed to study the effect of the tropospheric fluctuations on GPS phase signals (Schön and Brunner 2008b) is presented. The flexibility of the Mátern family will be highlighted as well as the possibility to improve in a manageable way the reliability and standard deviation of least-squares coordinate estimations by taking temporal correlations into account. Finally, an appendix gives necessary mathematical background on the Mátern covariance functions.

2 Physical background: atmospheric transmission and turbulence theory

2.1 Basic concepts—overview

The atmosphere can be considered as a medium varying randomly in time and space (Ishimaru 1997, chapter 17). Thus, GPS satellite signals that propagate through the atmosphere have to be described by statistical methods. The troposphere (a layer between approximatively 0–10 km of altitude) and the ionosphere (85–500 km of altitude) are the most important parts of the atmosphere to be considered for GPS transmission (Wheelon 2001, chapter 2). Frequency-dependent ionospheric effects due to the ionization by solar radiation can mainly be canceled via ionosphere-free linear combination. However, the troposphere being a non-dispersive medium, whether double differencing neither linear combination of observations eliminate its refractive effects on GPS phase measurements.

Turbulence, particularly in the boundary layer between 0–2 km height, is a fundamental phenomena in the troposphere and remains an actual research field. As examples, we cite here the wavelet approach by Khujadze et al. (2013), Farge (1992) or the large Eddy simulation (2008). From the point of view of GNSS signals, turbulence causes variations of the refractive index, that act on phase measurements, causing tropospheric slant delay fluctuations.

The turbulent troposphere can be modelized as a superposition of eddies or "swirl of motion" of different sizes, from the millimeter to the kilometer level depending on the altitude (Stull 2009; Wheelon 2001; Coulman and Vernin 1991); eddies and the surrounding atmosphere having different refractive indices. Thus, with this model in mind, we can motivate sources of correlations for GNSS observations using a geometric optics model: rays that are closer (temporally or spatially) encounter nearly identical eddies and are correlated together. Figure 1 proposes a schematic representation of the troposphere where eddies of different size and energy coexist, from small and isotropic in the boundary layer, the so-called 3D turbulence, to elongated, anisotropic in the loosely called free troposphere (Stull 2009).

In the boundary layer characterized by a high Reynolds number, strong turbulence occurs due to the influence of the Earth and the water vapor content; changes in the refractive index are rapid and eddies are small and isotropic (Coulman and Vernin 1991; Hunt and Morrison 2000). The energy cascade (Kolmogorov 1941) models the transfer and associated breakdown of eddies at a constant rate. Above the boundary layer, in the loosely called free atmosphere ($H > 1{,}000$ m) the turbulence is more 2D-like and the validity of the energy cascade which represents eddies breaking from large to small scales is questionable (Gage 1979).

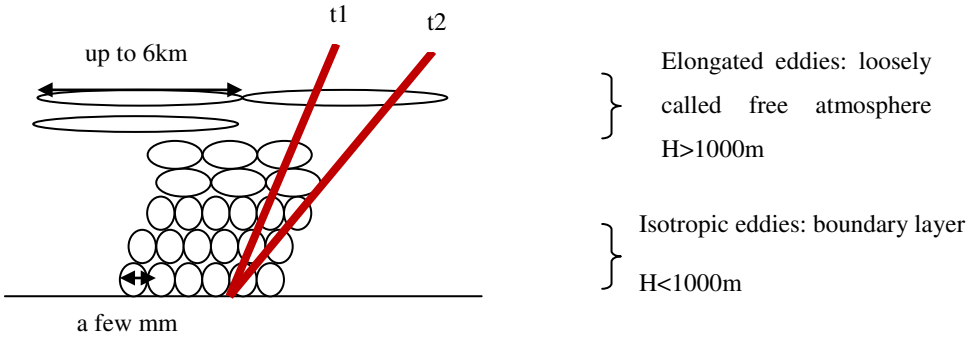

Fig. 1 Schematic representation of the troposphere seen from a satellite signal (adapted from Wheelon (2001, p83) based on measurements of the outer scale)

An important parameter for tropospheric turbulences is the structure constant C_n^2, which is a kind of measure of the intensity of turbulence; see for example Nilsson and Haas (Nilsson and Haas 2010) for a description of how this parameter can be evaluated. A typical profile for microwave C_n^2 in the troposphere (Wheelon 2001, p68) shows a decrease with height from approximately $10^{-14}\,\mathrm{m}^{-2/3}$ at 1,000 m altitude to $10^{-17}\,\mathrm{m}^{-2/3}$ at 7,000 m. However, the values are remaining in a range of 5.10^{-14}–$10^{-15}\,\mathrm{m}^{-2/3}$ between 1,000–3,000 m. Thus and following Wheelon (2001, chapter 2), for a GPS ray that propagates through the whole atmosphere, the free troposphere from 1,000 m up to 3,000 m will play a much more important role than the boundary layer below 1,000 m in creating correlations between phase GPS measurements. The intensity of turbulence is large enough and at the same time the reorganization is slower than at a lower altitude making the medium more stable.

This intuitive result can also be explained by considering the weak fluctuation mathematical approximation (Ishimaru 1997, chapter 17). The dielectric constant ε of the troposphere depends on the position $\mathbf{r}$ and time t and is expressed in a first-order approximation: $\varepsilon(\mathbf{r}, t) = n^2(\mathbf{r}, t)$, where n is the refractive index. Under this approximation, the covariance function for phase at a plane $x = L$ can be expressed by means of a filter function (Ishimaru 1997, p352):

$$C_\varphi(L, r) = 2\pi^2 k^2 L \int_0^\infty \kappa \mathrm{d}\kappa J_0(\kappa r) f_\phi(\kappa) \Phi_n(\kappa), \tag{1}$$

with J_0 the ordinary Bessel function of 0th order, $\Phi_n(\kappa)$ the 3D power spectrum of refractivity fluctuations for an homogenous medium independent of the location, $\kappa = \frac{2\pi}{L}$ the wavenumber, L the scale length and finally k the electromagnetic wavenumber. The function

$$f_\varphi(\kappa) = 1 + \frac{\sin(\kappa^2 L/k)}{\kappa^2 L/k} \tag{2}$$

can be considered as a filter function of the spectrum (Fig. 2).

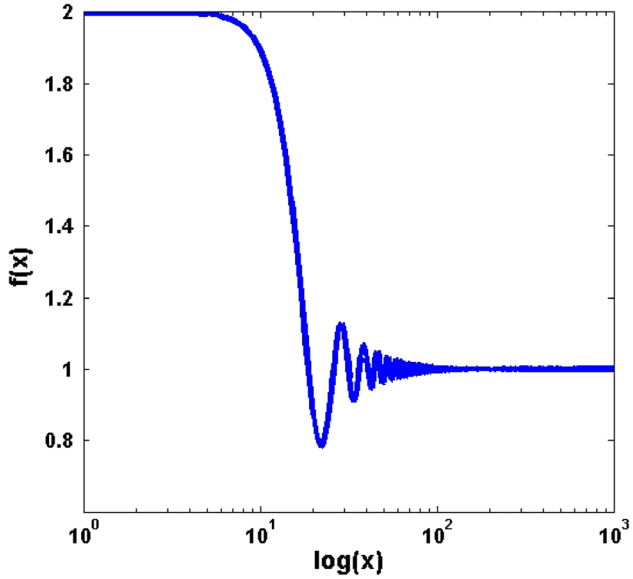

Fig. 2 Filter function $f_\varphi(x)$ versus $\log(x)$. For $x < 1$, the filter function is having nearly constant values close to 2

The region $\kappa < \frac{\sqrt{2\pi}}{\sqrt{\lambda L}}$ is strongly emphasized, meaning that larger eddies are more affecting the phase measurements than smaller ones. Since for GNSS signals $\lambda \approx 20\,\mathrm{cm}$, we will have $\frac{L_0^2}{\lambda} \approx 10^9 >> H$, where L_0 is the correlation length (in the free troposphere, i.e. the outer scale length $L_0 \approx 6{,}000\,\mathrm{m}$ for horizontal direction, $L_0 \approx 70$ m for vertical direction) and H is approximately the height of the troposphere (5,000–10,000 m).

The covariance function for phase measurement can be further simplified to:

$$C(L, r) = 4\pi^2 k^2 L \int_0^\infty \kappa \mathrm{d}\kappa J_0(\kappa r) \Phi_n(\kappa). \tag{3}$$

However, a further integration is not possible without knowledge of the power spectrum of the atmospheric fluctuations, which is a weighting function of the wavenumber κ.

From dimensional analysis, Kolmogorov (1941) has shown that the energy spectrum of turbulence should follow

a power law. The related velocity power spectrum as well as the power spectrum of passive scalars such as temperature or refractive index (Monin and Yaglom 1975) can be written as:

$$\Phi_n(\kappa) = \frac{0.033\, C_n^2}{(\kappa_x^2 + \kappa_y^2 + \kappa_z^2)^{11/6}}, \tag{4}$$

where C_n^2 is the structure constant. C_n^2 differs for optical and microwave measurements; microwave being more influenced by water vapor content and optical frequencies by temperature fluctuations. The vector of 3D wavenumbers is $\kappa = [\,\kappa_x\ \kappa_y\ \kappa_z\,]^{\mathrm{T}}$. This model is valid in the inertial range for homogeneous and isotropic turbulence, where $\frac{2\pi}{L_0} \leq \kappa \leq \frac{2\pi}{l_0}$ with L_0, l_0 being the outer and inner scale length of turbulence that bounds the inertial range, respectively.

However, this model yields infinite values for some quantities such as the mean square fluctuations of the refractive index $\langle(\delta n)^2\rangle$. As a consequence, the empirical Von Karman Model is often preferred:

$$\Phi_n(\kappa) = \frac{0.033\, C_n^2}{(\kappa_x^2 + \kappa_y^2 + \kappa_z^2 + \kappa_0^2)^{11/6}}, \quad \kappa_0 = \frac{2\pi}{L_0}. \tag{5}$$

Please refer to Voitsekhovich (1995) or Wheelon (2001, chapter 2) for a presentation of further models such as the Greenwood model or the exponential model.

Although only developed for the inertial range and isotropic turbulence, the Von Karman power law model has shown to be valid beyond these limits, particularly for 2D turbulence (Wheelon 2001; Kraichnan 1974). We will therefore make use of it.

2.2 Anisotropy, inhomogeneity

Isotropy and homogeneity are the main assumptions of the Kolmogorov model. However, GNSS phase measurements are especially affected by the propagation through the free atmosphere where eddies are mainly elongated. Inhomogeneity as well as anisotropy have to be taken into account in the power spectrum model.

Inhomogeneity

The troposphere can be considered in a first approximation as a locally inhomogeneous field with smoothly varying mean characteristics. Inhomogeneity can be expressed by a product of a slowly varying function which describes the spectral distribution of turbulent fluctuations for the whole medium $\Phi_{n,0}(\kappa)$ and a term with faster variations $C_n^2\left(\frac{\mathbf{r_1}+\mathbf{r_2}}{2}\right)$ describing the intensity of the fluctuations for the refractive index in a given region of the medium where $\mathbf{r_1}$ and $\mathbf{r}_2$ denote two different position vectors (Tatarskii 1971, p36). Thus, for different regions separated beyond the outer scale length, the power spectrum reads:

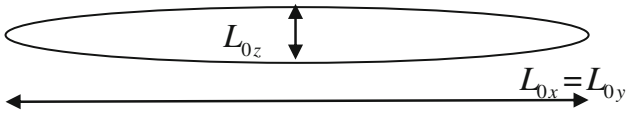

Fig. 3 Elongation of eddy

$$\Phi_n\left(\boldsymbol{\kappa}, \frac{\mathbf{r_1}+\mathbf{r_2}}{2}\right) = C_n^2\left(\frac{\mathbf{r_1}+\mathbf{r_2}}{2}\right)\Phi_{n,0}(\boldsymbol{\kappa}). \tag{6}$$

Anisotropy

As seen in Fig.1, horizontal elongated eddies of the free atmosphere are impacting the phase measurements. Following Wheelon (2001), the wavenumber spectrum can be expressed by:

$$\Phi_n(\boldsymbol{\kappa}) = abc\,\Phi_n\left(\sqrt{a^2\kappa_x^2 + b^2\kappa_y^2 + c^2\kappa_z^2}\right), \tag{7}$$

where a,b,c are stretching factors describing the elongation of the eddies in the three dimensions, i.e. $L_{0x} = aL_0$, $L_{0y} = bL_0$, $L_{0z} = cL_0$. $L_{0x} = L_{0y}$ are the horizontal elongations and L_{0z} the vertical one.

Figure 3 is a schematic representation of an horizontal elongated eddy corresponding to the layered turbulence above the planetary boundary layer, in the loosely called free troposphere where the effects of the Earth's surface friction on the air motion are becoming negligible. The outer scale length's value is between 6,000 and 10,000 m (please refer to Wheelon 2001, chapter 2 for results of experiments of the Global Atmospheric Sampling Program). The vertical elongation is 100 times smaller and between 10 and 70 m, the higher values being measured at an altitude around 1,000 m (five years campaign New Mexico, Wheelon 2001 p83).

2.3 Taylor's frozen hypothesis

To access to the temporal covariance of phase measurements $C(t) = \langle\varphi(t), \varphi(t+\tau)\rangle$, τ being a time increment, the Taylor's frozen hypothesis (Taylor 1938) is assumed. It postulates that the phase covariance between two instants separated by τ is identical to the spatial covariance of phase measurement at two stations separated by a vector $\mathbf{r} = \mathbf{u}\tau$, where $\mathbf{u}$ is the mean wind vector. Thus, the atmosphere is said to be "frozen" during the measurement, eddies are only moved by the mean wind $\mathbf{u}$. A value of $\|\mathbf{u}\| = 8\,\mathrm{ms}^{-1}$ seems relevant (Stull 2009).

This approximation performs better as the mean wind speed increases. In the case of GPS phase covariance at synoptic scales, the geostrophic wind which blows parallel to the isobar can be chosen (Wheelon 2001, chapter 6). Thus, the covariance (Eq. 3) can be written as $C(\tau) = 4\pi^2 k^2 L \int_0^\infty \kappa\,\mathrm{d}\kappa\, J_0(\kappa\tau u)\,\Phi_n(\kappa)$ where it is assumed that the wind vector does not change with time and position and the satellite geometry varies slowly with time.

3 Formulation of the new covariance model

3.1 Formulation of the temporal covariance via spectral density

Following Wheelon (2001) and using the previous approximations as well as the von Karman spectrum for the refractivity fluctuations expressed in stretched coordinates, the spectrum of phase measurements $W_{\varphi_i}(\omega)$ can be obtained by integrating along the lines-of-sight:

$$W_{\varphi_i}(\omega) = 2.192H\frac{k^2C_n^2ca^{-5/3}u^{5/3}}{\sin^2(El_i)}\frac{1}{\left[\omega^2+\left(\frac{\kappa_0 u}{a}\right)^2\right]^{4/3}}, \quad (8)$$

where El_i is the elevation of the satellite i, H the tropospheric deep or height, $a = b$ and $c$the horizontal and vertical stretched parameters for the outer scale length, ω is the angular frequency and u the wind velocity.

A rational spectral density can be recognized. The considered process being 1D (only a time dependency), the previous formula can be reformulated, introducing the dimensionality $D = 1$:

$$W_{\varphi}(\omega) = 2.192H\frac{k^2C_n^2ca^{-5/3}u^{5/3}}{\sin^2(\mathrm{El})}\frac{1}{[\omega^2+\alpha^2]^{5/6+1/2}}, \quad (9)$$

where $\alpha = \frac{\kappa_0 u}{a}$ and $\nu = \frac{5}{6}$ $\left(\nu + \frac{D}{2} = \frac{4}{3}, D = 1\right)$. Using the equivalence of Appendix A (Rasmussen and Williams 2006) and the Wiener–Khinchin theorem, the covariance is a so-called Mátern covariance function which reads:

$$C_{\varphi_i}(t, t+\tau) = 0.7772\frac{k^2HC_n^2c\kappa_0^{-5/3}}{\sin(\mathrm{El}_i(t))\sin(\mathrm{El}_i(t+\tau))} \times\left(\frac{\kappa_0 u\tau}{a}\right)^{5/6}K_{5/6}\left(\frac{\kappa_0 u\tau}{a}\right), \quad (10)$$

with a smoothness parameter of $\nu = 5/6$ and a Mátern correlation time $1/\alpha$, $\alpha = \frac{\kappa_0 u}{a}$. Equation (10) is a closed formula and thus free of integrals. Moreover, the identification as Mátern covariance opens up new interpretations (cf. Appendix A). Due to the use of the von Karman power spectrum, the continuity at the origin is not given. A formulation of the variance can be found in Wheelon (2001, p164) or using the limit of the Bessel function (Abramowitz and Segun 1972):

$$\lim_{\tau->0}K_{5/6}(\tau) = \frac{1}{2}\Gamma\left(\frac{5}{6}\right)\left(\frac{2}{\tau}\right)^{\frac{5}{6}}\left(1-\tau^{\frac{5}{3}}\frac{\Gamma\left(\frac{1}{6}\right)}{\Gamma\left(\frac{11}{6}\right)}....\right)$$

yielding

$$C_{\varphi_i}(t,t) = 0.782\frac{k^2HC_n^2c\kappa_0^{-5/3}}{\sin^2(El_i(t))}. \quad (11)$$

Approximations

Until now, following approximations were made to express the covariance structure of GPS phase signals propagating through the turbulent free troposphere:

- No dependency of the structure constant with height is taken into account. The constant value of $5.10^{-14}\,\mathrm{m}^{-2/3}$ was taken. Following Treuhaft and Lany (1987), for simplification and homogeneity, a constant value should be enough as proposed by Schön and Brunner (2008a), Wheelon (2001). If more accuracy is needed, profiles of the structure constant for microwave could be used as well as a layered model (Kleijer 2004; Gradinarsky 2002).
- No dependency of the outer scale length with height is assumed. It is very difficult to access the structure of the horizontal outer scale length. Range of values between 6,000 and 10,000 m has been experimentally determined in the free atmosphere, cf. Wheelon (2001).
- Following Wheelon (2001, chapter 4), only the turbulence in the free atmosphere and not in the boundary layer is taken into account. However, by changing the outer scale length to $L_0 = 100-600$ m and the value of H and the structure constant C_n^2 accordingly, our model can be extended to the boundary layer. In this case, the Mátern correlation time is more than 10 times smaller than for the free atmosphere case.
- The wind speed is taken constant which is a good approximation above 1,000 m under normal meteorological condition; cf. Wheelon (Wheelon 2001, chapter 6) for wind fluctuations.
- Taylor's Frozen Hypothesis is assumed. This approximation should be valid as long as the GPS lines-of-sight are not too far from each other. Thus, the model for computing the phase covariance between two different satellites should be carefully used if the distance between two rays at approximately $H = 1{,}000-2{,}000\,m$ is larger than 10 km (the maximal outer scale length in the atmosphere, Wheelon 2001) since the turbulence at such scales is not a priori having a Kolmogorov behavior.
- This model assumes a flat atmosphere using a $\frac{1}{\sin(\mathrm{El})}$ mapping which is a good approximation for high elevation angles. However, for lower elevation angles (below 10°), more elaborated tropospheric mapping functions should be used for more accuracy (Böhm and Schuh 2013).

3.2 Dependencies and parameter sensitivity

3.2.1 General remarks

Several tropospheric parameters are involved in the proposed model. Thus, in a next step, the physical dependencies are studied, leading to a proposal for modeling the phase correlations between GPS signals of two different satellites.

Four parameters coming from the turbulence theory have a scaling effect on the variance and covariance: the tropospheric height H, the structure constant C_n^2, the vertical elongation parameter $c$of the stretched coordinates, and the

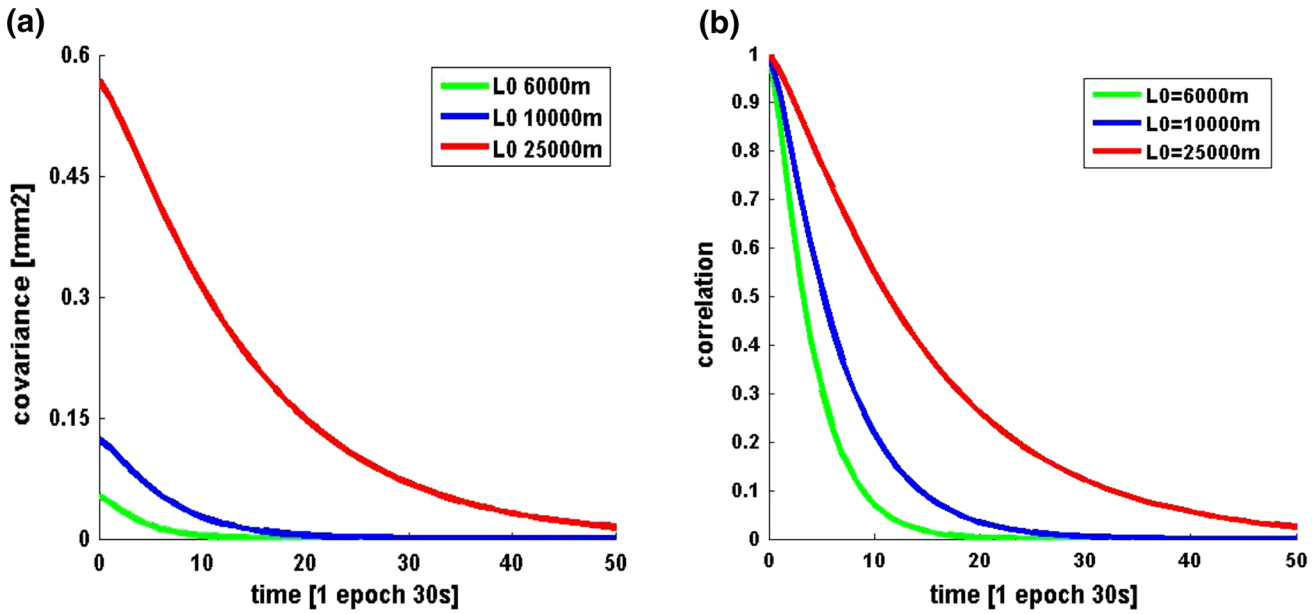

Fig. 4 Covariance (**a**) and correlation function (**b**) by varying the outer scale length from 6,000 to 25,000 m. A satellite at low elevation (15°) was taken for the simulation as well as $c = 0.01$, $C_n^2 = 5.10^{-14}\,\mathrm{m}^{-2/3}$, $u = 8\,\mathrm{ms}^{-1}$

outer scale length $\kappa_0 = \frac{2\pi}{L_0}$. In addition, both the wind velocity and the outer scale length are also acting on the Mátern correlation time (CT) via $\alpha = \frac{\kappa_0 u}{a}[\mathrm{s}^{-1}]$, which we reduce to $\alpha = \kappa_0 u$ by taking $a = 1$ and an horizontal elongation of $L_0 = 6{,}000\,\mathrm{m}$. Thus, since $a/c = 1/c > 100$ can be assumed in the free troposphere, c will be set to 0.01.

If a geostropic wind value between 8–10 $\mathrm{ms}^{-1}$is taken as well as an outer scale length of 6,000–10,000 m, the typical range of values of α should be $0.005-0.01\ \mathrm{s}^{-1}$, i.e. the correlation time as defined in El-Rabbany (1994) is between 100–200 s.

In the following, the impact of different values of the parameter (outer scale length and wind velocity) on the covariance is exemplary studied.

3.2.2 Changing the outer scale length L_0

In Fig. 4, the outer scale length parameter was changed from 25 km (very elongated eddies, synoptic scales) to 6 km, which should be considered as a reference value (Wheelon 2001) for the GPS temporal phase covariance. For a better comparison, the same value of the structure constant was used for the three cases.

A large value of the outer scale length (red 25 km) leads to a longer Mátern correlation time (CT) and larger values of the covariance. A standard value of 6 km results in a shorter Mátern CT as well as smaller covariance. Acting on both the correlation time and the variance, the outer scale length determines the behavior of the spectrum at low frequencies.

3.2.3 Changing the wind velocity

In Fig. 5, we changed the wind velocity from 4 to 10 ms^{-1}. The variance does not depend on this parameter, thus only the Mátern correlation time $1/\alpha$[s] will change. For large values of the wind speed, the Mátern CT is shorter than for small values (here $4\,\mathrm{ms}^{-1}$) for which the spectral energy is shifted at low frequencies. Values between 8 and $10\,\mathrm{ms}^{-1}$ should be physically most relevant (blue and green line) corresponding to the approximate value of the geostropic wind (Stull 2009). Moreover, working under Taylor's hypothesis, higher values of the wind speed are preferable.

3.3 Extended formulation of the covariance—case two satellites—one or two stations

We propose to extend the "one satellite-one station" covariance model to the case when the covariance between two phase measurements of different satellites i and j at different stations A and B is needed. The case "two satellites, one station" is given by taking A = B in the following formula. Our development is based on the observations that the correlations times of GPS phase measurements are typically 3–7 min (Schön and Kutterer 2006). During that time, the satellite geometry is only little varying and a decomposition into a temporary fixed satellite geometry at a time t and temporal variations seems adequate. Consequently, both temporal and spatial correlations are taken into account.

At a given height $H = 1{,}000\,m$ (tropospheric height), and for one epoch when satellite i and j are present, the paths of

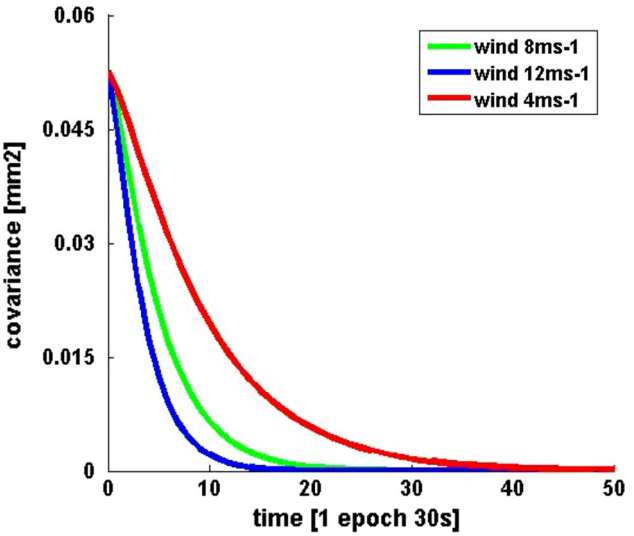

Fig. 5 Covariance functions by varying the wind velocity from 4 to 12 ms^{-1}. $c = 0.01$, $C_n^2 = 5.10^{-14}\,\mathrm{m}^{-2/3}$, $L_0 = 6{,}000$ m and a satellite at low elevation (15°) were taken for the simulation

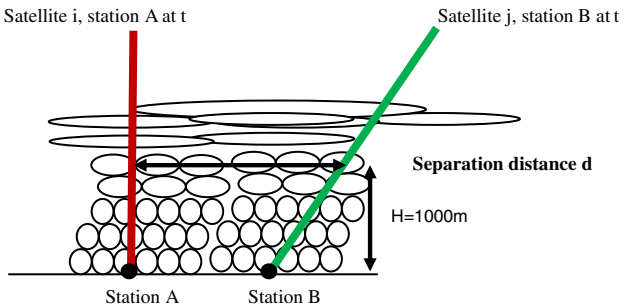

Fig. 6 Simplified version of the concept of separation distance at t (Schön and Brunner 2008a)

satellite i and j are separated by a distance called the "separation distance" $d_{t,H=1{,}000\,\mathrm{m}}$ which depends on the geometry (elevation, azimuth) of the two satellites at a given time (Schön and Brunner 2008a). The following figure (Fig. 6) illustrates in a simple way the concept of separation distance. More details can be found in Schön and Brunner (2008a).

No influence of the wind vector with time on the separation distance (Schön and Brunner 2007) is here taken into account since the separation distance is computed at one epoch. A special case occurs for separation distance larger than the maximum outer scale length of the troposphere (approximately 10 km, Wheelon 2001, p82). Indeed, neither the Kolmogorov law nor the Taylor's frozen hypothesis should be applied. For this particular case, correlations due to tropospheric turbulences can be neglected since the rays are considered too far away from each other. Thus, the procedure can be summarized as follow:

First step: Compute the separation distance $d_{t,H=1{,}000\,\mathrm{m}}$

Second step: If $d_{t,H=1{,}000\,\mathrm{m}} < 6{,}000$ m, set $L_0 = 6{,}000$ m.

If $6{,}000\,\mathrm{m} < d_{t,H=1{,}000\,\mathrm{m}} < 10{,}000$ m, the outer scale length is taken to $L_0 = d_{t,H=1{,}000\,\mathrm{m}}$. The vertical elongation is 100 times smaller than the horizontal one (Wheelon 2001, chapter 2). Thus, for high values of the separation distance, the correlations between microwave phase measurements will come from longer eddies, that appear at higher altitudes in the free troposphere. The structure constant should be taken accordingly smaller than for the case "one satellite". Following the previous mentioned structure constant profile (Wheelon 2001, chapter 2) we propose to take approximately the structure constant by a factor 10 lower as for the previous case $C_n^2 = 5.10^{-15}\,\mathrm{m}^{-2/3}$.

As a consequence, the covariance between two phase measurements of two different satellites (i, j) is given by:

$$\begin{cases} \text{if} \quad d < 6{,}000\,\mathrm{m} : \langle \varphi_A^i(t), \varphi_B^j(t+\tau) \rangle \\ \quad = \ldots 0.7772 \frac{k^2 H C_n^2 c}{\sin(\mathrm{El}_i^A(t)) \sin(\mathrm{El}_j^B(t+\tau))} \left(\frac{2\pi}{L_0}\right)^{-5/3} \\ \qquad \left(\frac{2\pi u \tau}{L_0 a}\right)^{5/6} K_{5/6}\left(\frac{2\pi u \tau}{L_0 a}\right) \\ \text{if} \quad 6{,}000 < d < 10{,}000\mathrm{m} : \langle \varphi_A^i(t), \varphi_B^j(t+\tau) \rangle \\ \quad = \ldots 0.7772 \frac{k^2 H C_n^2 c}{\sin(\mathrm{El}_i^A(t)) \sin(\mathrm{El}_j^B(t+\tau))} \left(\frac{2\pi}{d_{t,H=1{,}000\,\mathrm{m}}}\right)^{-5/3} \\ \qquad \left(\frac{2\pi u \tau}{d_{t,H=1{,}000\,\mathrm{m}} a}\right)^{5/6} K_{5/6}\left(\frac{2\pi u \tau}{d_{t,H=1{,}000\,\mathrm{m}} a}\right) \\ \text{if} \quad d > 10{,}000\,\mathrm{m} : \langle \varphi_A^i(t), \varphi_B^j(t+\tau) \rangle = 0 \end{cases} \tag{12}$$

As previously, the wind speed u is taken to its geostropic value. For longer observation spans, different time t may be used.

As the separation distance is replacing the outer scale length in this new model, the behavior of the covariance versus time is the same as in Fig. 4. Typical values of the separation distance at $H = 1{,}000$ m depends on the satellite geometry (azimuth and elevation) and are between a few hundred meters to 10,000 m or more.

The rational spectral density of phase measurements allowed us to propose a new and simple model for the computation of GPS phase covariance based on the Mátern covariance family. Inhomogeneity as well as anisotropy and non-stationarity were taken into account and reflect the physical effects of the atmosphere on GPS signals. Moreover, by allowing a great flexibility through the smoothness and the correlation time parameters which can be changed if needed and estimated via likelihood estimation (Stein 1999; Handcock and Wallis 1994), such covariance functions are quite promising for modeling temporal correlations, not only tropospheric correlations as proposed in the paper but also multipath or receiver-related internal correlations.

Amplitudes fluctuations, which are affected by small eddies, do not allow the geometrical–optical approximations valid for microwave signals and diffraction theory has to be used (Ishimaru 1997, chapter 17). As a consequence, the pro-

posed model is not adequate for modeling the tropospheric temporal correlation of amplitude measurements.

3.4 Comparison with other covariance models

Other models for GPS temporal correlations have been proposed in the past such as the exponential model, the Treuhaft and Lanyi model (1987) or the Schön and Brunner (2008a) model. In this section, the differences and similarities of these models are shortly described.

3.4.1 Exponential model

Proposed by El-Rabbany (1994), the exponential model was concretely used exemplary by Howind et al. (1999) and Radovanovic (2001) to describe temporal correlations. A direct link to tropospheric correlations is not explicitly given. However, it is a special case of the Mátern family with a smoothness parameter of 1/2 (see Appendix A for more details). Consequently, this model is close to our proposal with $\nu = 5/6 \approx 0.833$. Moreover, the correlation time as defined by Howind et al. (1999) was taken constant between 100–300 s, empirically chosen by data analysis. In our proposal, the Mátern correlation time, although not directly corresponding to the correlation time, varies approximately in the same range. Moreover, it depends on atmospheric conditions (wind, outer scale length) allowing the computation of the covariance for phase measurements of two different satellites.

3.4.2 ARIMA processes

In geodesy (see exemplary Grafarend 1976), the so-called first autoregressive Markov model is often used to model correlations. It corresponds to a smoothness parameter of 1, which is also close to the $\nu = 5/6 \approx 0.833$ given by turbulence theory. Jansson and Persson (2013) fitted a covariance function with this smoothness factor of 1 to GPS observations.

Continuous ARIMA processes have a rational spectral density (Rasmussen and Williams 2006). Luo et al. (2012) made use of ARIMA(p, q) procedure to decorrelate least-squares residuals. They showed that some values of p and q perform better than others depending on the stations (for instance on the influence of multipath). Such models are however empirical and the corresponding covariance functions are mathematically more complicated to express than the Mátern one (see exemplary Jones and Vecchia 1993).

3.4.3 Treuhaft and Lany model

Treuhaft and Lany (1987) (TL) proposed a turbulence-based VCM for tropospheric delays in VLBI. This model is used by Nilsson and Haas (2010), Pany et al. (2011) or Romero-Wolf et al. (2012) for simulations or real data analysis of VLBI measurements.

The covariance between two tropospheric slant delays t_1, t_2 reads:

$$C_\varphi(t_1,t_2) = \frac{1}{\sin(\mathrm{El}_1)\sin(\mathrm{El}_2)}\left(H^2\sigma^2 - \frac{1}{2}\int_0^H\int_0^H \mathrm{d}z\mathrm{d}z' \times D_n\left(\frac{\left|\mathbf{s}_1(z) - \mathbf{s}_2(z') - \langle\mathbf{u}\rangle\Delta t\right|}{\sin(\mathrm{El})}\right)\right), \tag{13}$$

where $\langle\mathbf{u}\rangle$ is the mean wind velocity, $\mathbf{s}_1$ and $\mathbf{s}_2$ denote the line-of-sight vectors, σ^2 the variance of the wet refractivity fluctuations which is assumed independent of $\mathbf{s}$. It can be expressed by $\sigma^2 = \frac{1}{2}D_n(r)$ as $r \to \infty$, assuming that the troposphere parameters are completely uncorrelated. Built on a modified version of the Kolmogorov structure function for the refractive index, $D_n(r) = C_n^2\frac{r^{2/3}}{1+(\frac{r}{L})^{2/3}}$, this covariance model leads to a double integral which must be solved numerically. Furthermore, Eq. (13) is based on the relation $C_\varphi(t, t+\tau) = \frac{1}{2}(D_\varphi(\infty) - D_\varphi(\tau))$ valid only for a stationary process, where D_φ is the phase structure function computed by directly integrating the modified version of the Kolmogorov structure function of the refractive index along the lines-of-sight. The parameter L, chosen in physically reasonable range, was taken to 3,000 km, a value at which empirical structure functions, for VLBI data saturate for large values of r.

In the TL proposal, neither anisotropy nor inhomogeneity was taken into account. Moreover, this model is based on a double integral which can only be solved numerically, necessitating a large computational effort.

3.4.4 Schön and Brunner covariance model

Schön and Brunner (2008a) developed a covariance model based on the time-dependent integrated separation distance d:

$$\begin{aligned}\langle\varphi_A^i(t),\ \varphi_B^j(t+\tau)\rangle &= \frac{12}{5}\frac{0.033}{\Gamma\left(\frac{5}{6}\right)}\frac{\sqrt{\pi^3}\kappa_0^{-2/3}2^{-1/3}}{\sin\mathrm{El}_i^A\sin\mathrm{El}_j^B}C_n^2\int_0^H\int_0^H(\kappa_0^d)^{1/3}K_{1/3}(\kappa_0^d)\mathrm{d}z_1\mathrm{d}z_2\\ &= \frac{2^{1/3}}{3\Gamma\left(\frac{2}{3}\right)}\frac{\kappa_0^{-2/3}}{\sin\mathrm{El}_i^A\sin\mathrm{El}_j^B}C_n^2\int_0^H\int_0^H(\kappa_0^d)^{1/3}K_{1/3}(\kappa_0^d)\mathrm{d}z_1\mathrm{d}z_2\end{aligned} \tag{14}$$

The parameters H, κ_0, c are the same as previously described. Not only the wind velocity but also the wind orientation

(wind vector) is involved in the computation of the separation distance d, and the model can therefore be considered as a 2D one. A double integrated Mátern kernel with $\nu = \frac{1}{3}$ is obtained. However, for the case "one satellite" where the geometries are slowly varying with time, it will lead as in our previous formulation to a spectral density with a power law dependence of $\frac{4}{3}$ since $\nu + \frac{D}{2} = \frac{4}{3}$ with $\nu = \frac{1}{3}$, $D = 2$, D being the dimensionality (Appendix A). Thus the two formulations (Eqs. 14, 10) are equivalent for the GPS phase covariance for one satellite.

Schön and Brunner (2008a) proposed a direct integration for the variance which reads:

$$\langle \varphi^2 \rangle = \frac{12}{5} \frac{0.033}{\Gamma\left(\frac{5}{6}\right)} \frac{\sqrt{\pi^3} \kappa_0^{-2/3} 2^{-1/3}}{(\sin \mathrm{El})^2} C_n^2 H^2 \times \left\{ \frac{\pi 2^{1/3}}{\sqrt{3}\,\Gamma\left(\frac{2}{3}\right)} {}_2F_3\left(\left[\frac{1}{2}, 1\right], \left[\frac{2}{3}, \frac{3}{2}, 2\right], \frac{z^2}{4}\right) - \frac{27}{80} 2^{2/3} \Gamma\left(\frac{2}{3}\right) z^{2/3}\, {}_1F_2\left(\left[\frac{5}{6}\right], \left[\frac{11}{6}, \frac{7}{3}\right], \frac{z^2}{4}\right) \right\}, \tag{15}$$

where F denotes the hypergeometric function (Abramowitz and Segun 1972). The dimensionless argument z is given by $z = \frac{p \kappa_0 H}{\sin \mathrm{El}}$, where the factor p describes the impact of anisotropy on the variance. For small values of c, the variance should be replaced using the small argument approach (Eq. 11)., since the hypergeometric function (Eq. 15) takes rapidly high values, leading to computational issues by taking the difference of the two hypergeometric functions.

Schön and Brunner (2008a) computed the separation distance for a more general case by allowing a time dependency through the wind vector. As a consequence, this model is more general than our proposal. However, no dependency of the outer scale length with the separation distance or of the structure constant with the outer scale length is proposed. Moreover, for some satellite geometry, the maximum of covariance is not at the first epoch but "delayed". Such a behavior is physically difficult to understand when considering the rapid reorganization of the troposphere. The corresponding covariance matrices may be not positive definite anymore. Moreover, considering anisotropy for the turbulence parameters of interest ($c = 0, 01$, $L_0 = 6{,}000$ m) some numerical instabilities due to the double integral occur.

Thus our simplification for the case two satellites-one or two stations, allowing both a rapid computation and a physical interpretation, should be preferred.

4 Case study

In the following part, the influence of our model on the coordinate estimates in least-squares adjustments as well as the influence of Mátern parameters (smoothness and Mátern correlation time) will be studied. We aim to validate the physically derived smoothness factor and Mátern correlation time presented in Sect. 3.1. Fully populated covariance matrices are computed with the previous formulas and implemented in a weighted least-squares model. After a short presentation of the methodology used, the results for the repeatability as well as for the quadratic deviation of the batch coordinates will be discussed.

4.1 Least-squares solution

We use the Seewinkel Network (Schön and Brunner 2008b) specially designed to study the temporal correlations due to turbulence on GPS measurements. It consists of six exactly aligned stations P0, P1, P2, P4, P8, and P16 with separation of approximately 1, 2, 4, 8, and 16 km, respectively. It was measured on April, 15th 2003 during 8h (5:45–13:45 GPS time) using identical equipment, a 1Hz data rate, and a cutoff-angle of 3°. Multipath is weak, thus the correlations are assumed to come principally from tropospheric fluctuations.

The coordinates of the first station P0 were held fixed and double differences were formed. Ambiguities were precomputed. The North, East and Up (N, E, U) components of P1 and P8, respectively, were estimated for the baseline: P0P1 (1,000 m) as well as the longer baseline P0P8 (8,000 m).

Since the observations can be assumed to be uncorrelated after 600s (Schön and Kutterer 2006), the whole observation period of 8 h is split into nonoverlapping batches of 600s. To analyze the impact of the stochastic model on the coordinate repeatability, two sampling rates are used: overall 45 batches à 20 epochs, 1 epoch = 30 s and 45 batches a 600 epochs, 1epoch = 1 s were computed in a weighted least-squares adjustment. No tropospheric parameters were estimated and the CODE reprocessing orbits and clocks were used (Dach et al. 2009). An apriori standard deviation of 1 mm was assumed for the L1 carrier phase measurements.

For each batch b, the coordinates are computed:

$$\hat{\mathbf{x}}_b = [\, N_b \;\; E_b \;\; U_b \,]^{\mathrm{T}} = (\mathbf{A^T P A})^{-1} \mathbf{A^T P y}, \;\; \text{with } \mathbf{P} = \mathbf{Q}_{\mathrm{DD}}^{-1}, \tag{16}$$

$\mathbf{Q}_{DD}$ is the cofactor matrix of the double difference observations, thus $\mathbf{Q_{DD}} = \mathbf{M^T Q M}$, $\mathbf{M}$ is the matrix of the mathematical correlation (Beutler et al. 1987), $\mathbf{Q}$ the positive-definite cofactor matrix of the undifferenced observations. $\mathbf{A}$ is the design matrix of each batch, $\mathbf{y}$ the vector of double differences.

The diagonal elements of the matrix $\widehat{\mathbf{\Sigma}}_{\mathbf{apost},b} = \widehat{\sigma}_0^2 (\mathbf{A^T P A})^{-1}$, $\widehat{\sigma}_0^2 = \frac{\mathbf{v^T Q_{DD}^{-1} v}}{n_b - 3}$ (n_b number of double differences for the batch b) are $\widehat{\sigma}_b^2 = [\, \widehat{\sigma}_{N,b}^2 \;\; \widehat{\sigma}_{E,b}^2 \;\; \widehat{\sigma}_{U,b}^2 \,]^{\mathrm{T}}$. They

represent the a posteriori variances of the unknowns. $\mathbf{v}$ is the residual vector of the least-square solution for the batch b.

The mean over all batches is computed leading to:

$$\hat{\sigma}_{i,\mathbf{apost}} = \frac{1}{m}\sum_{b=1}^{m}\hat{\sigma}_{i,b}, \tag{17}$$

where $i = \{N, E, U\}$ and m is the number of batches.

The quadratic deviation of the coordinates in [mm] reads

$$\delta_i = \sqrt{\frac{1}{m}\sum\nolimits_{b=1}^{m}\Delta\hat{x}_{i,b}^2},\ i = \{N, E, U\}, \tag{18}$$

$\Delta\hat{x}_{i,b}$ is the parameter deviation for the batch b of the estimated coordinates $\hat{N}, \hat{E}, \hat{U}$ and the reference values N_0, E_0, U_0 obtained from static positioning over the whole 8-h observation window.

For all coordinate components, their quadratic deviation δ_i is compared to the a posteriori variance $\hat{\sigma}_{i,\mathbf{apost}}$. The ratio $R_i = \frac{\hat{\sigma}_{i,\mathbf{apost}}}{\delta_i}$ is formed. It should be as close as possible to 1, meaning that no overestimation occurs (Rao and Toutenburg 1999). Both $\hat{\sigma}_{i,\mathbf{apost}}$ and δ_i are independent of the a priori variance factor (Kutterer 1999). Thus the cofactor matrices and not the covariance matrices will be used.

4.2 Methodology

For different cofactor matrices, the three parameters $\delta_i, \hat{\sigma}_{i,\mathbf{apost}}, R_i$ are determined. We compare our model to the results given by other smoothness and correlation time factors as well as to the typically used elevation-dependent weighting. In the following, we will call:

- EPS model, the elevation depending model with $\mathbf{Q} = \mathbf{Q}_\varepsilon$

$$\mathbf{Q}_\varepsilon(i,i) = \mathrm{diag}\left(\frac{1}{\sin^2(\mathrm{El}_i)}\right) \text{ with } \mathbf{Q}_\varepsilon(i,i) = 1 \text{ when } El_i = 90^\circ \tag{19}$$

- CORR model. In this case, the global cofactor matrix before mathematical correlations is given by

$$\mathbf{Q} = (1-\beta)\,\mathbf{Q}_{\mathbf{temp}} + \beta\mathbf{Q}_\varepsilon, \tag{20}$$

where $0 \le \beta \le 1$, called noise factor, is a positive parameter depending on the observations noise. Following Jansson and Persson (2013), β is defined as the ratio $\beta = \frac{\text{nugget}}{\text{sill}}$ of the structure function of the double difference observations. We found a mean value of $\beta = 0.3$ for double differences with low elevation satellites for the baseline length P0P1 and $\beta = 0.05$ for P0P8, meaning that relatively more high-frequency noise remains in the time series.

The temporal cofactor matrices $\mathbf{Q}_{\mathbf{temp}}$ are computed thanks to the Mátern covariance functions with a given smoothness factor and Mátern correlation time and scaled as Eq. 19. To check the influence of the variation of the Mátern parameters on the least-squares solutions, they were varied from 1/6 to 4/3 for the smoothness ν and $[10^{-3}-10^{-2}]\mathrm{s}^{-1}$ for α (inverse of the Mátern CT), respectively. The case $\nu = 1/2$ corresponds to the exponential case, while $\nu = 1$ is the AR(1) model (Appendix A). First values of the cofactor matrices were computed using the limit of the Bessel function (Abramowitz and Segun 1972) as shown in Eq. 11.

It follows that the two cofactor matrices $\mathbf{Q}$ and $\mathbf{Q}_\varepsilon$ have the same diagonal elements. Thus, the temporal cofactor matrices are not "underweighted" as long as the observation noise is not close to 1.

Note Other noise effects such as thermal noise (Radovanovic 2001; Schön and Brunner 2008b), are modeled in a first approximation by adding an elevation-dependent matrix to the Mátern temporal cofactor matrix $\mathbf{Q}_{\mathbf{temp}}$. A positive quantity added to the diagonal elements of the fully populated covariance matrix represents measurement errors or the so-called "nugget" effect in kriging (Cressie 1993). Moreover, this matrix yields a stabilization of the covariance matrices (Tikhonov et al. 1995). Although exemplary, Williams et al. (2004) modeled the covariance of GPS observations by adding a white noise covariance matrix (power spectrum of 0 corresponding to the identity covariance matrix) and a flicker noise matrix (e.g. power spectrum with a power law of -1), we chose not to add an identity matrix but to model the observations noise as elevation-dependent.

As we do not intend to compare the influence of different covariance models but only the influence of temporal correlations that gives an optimal quadratic deviation, the case where $\mathbf{Q} = \mathbf{I}$ which leads to poorer coordinate scatter and ratio than elevation-dependent models was not analyzed here.

4.3 Building the fully populated covariance matrices

Without loss of generality, we assume a satellite-by-satellite ordering scheme of the undifferenced GPS carrier phase observations. As a consequence, for one station A, the covariance matrix is built as follow:

$$\mathbf{C}_A^{i,j} = \begin{bmatrix} \sigma_{i1}^{j1} & \sigma_{i1}^{j2} & \sigma_{i1}^{j3} & \dots & \sigma_{i1}^{ju} \\ \sigma_{i2}^{j1} & \sigma_{i2}^{j2} & \sigma_{i2}^{j3} & & \sigma_{i2}^{ju} \\ & \dots & \dots & & \\ \sigma_{ik}^{j1} & & & & \sigma_{ik}^{ju} \end{bmatrix}$$

where σ_{ik}^{in} is the covariance between the satellite i at epoch k and satellite i at epoch n. The size of the covariance matrices for two different satellites is depending on the size of the

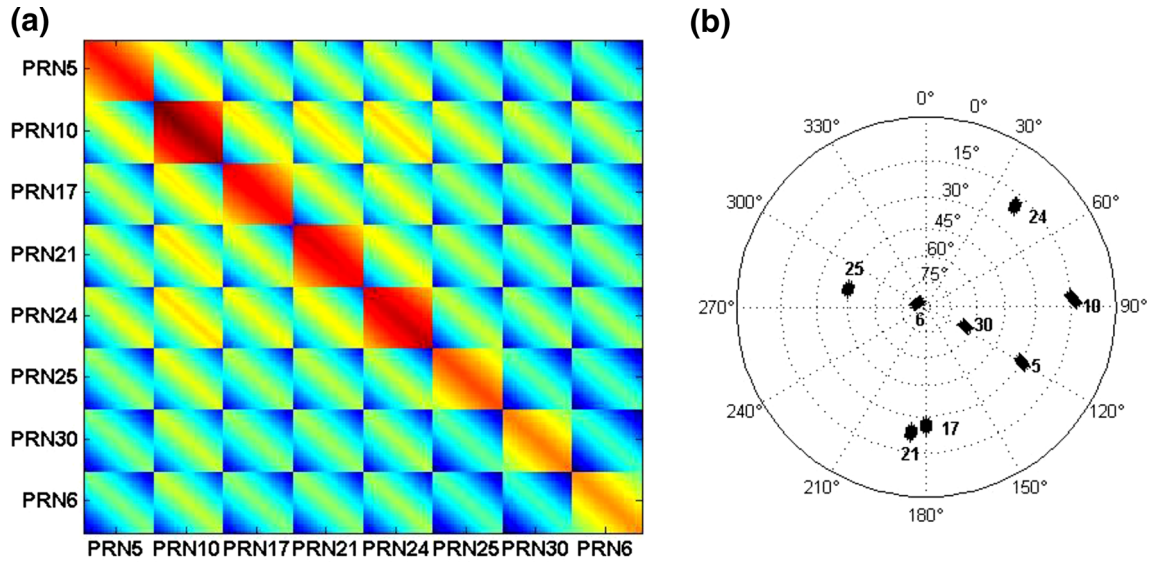

Fig. 7 **a** Example of the structure of the covariance matrix $\mathbf{C}_A$ for one station (log covariance values were plotted for more readability) and **b** the corresponding skyplot

elevation vectors: here for satellite i: k epochs and for satellite j: u epochs. It follows that the covariance matrix for the first station is given by:

$$\mathbf{C}_A^{=} \begin{bmatrix} \mathbf{C_A^{1,1}} & \mathbf{C_A^{1,2}} & \mathbf{C_A^{1,3}} & \dots & \mathbf{C_A^{1,n}} \\ & \mathbf{C_A^{2,2}} & \mathbf{C_A^{2,3}} & & \mathbf{C_A^{2,n}} \\ & \dots & \mathbf{C_A^{3,3}} & & \\ & & & & \mathbf{C_A^{n,n}} \end{bmatrix}$$

$\mathbf{C}_A$ is a symmetric positive-definite covariance matrix. The diagonal blocks $\mathbf{C}_A^{\mathbf{i},j}$ of $\mathbf{C}_A$ are also symmetric but not exactly Toeplitz due to the small non-stationarity of the model. For two stations, the global covariance matrix reads:

$$\Sigma_{\mathbf{temp}} = \begin{bmatrix} \mathbf{C}_A & \mathbf{C}_{A,B} \\ \mathbf{C}_{A,B} & \mathbf{C}_B \end{bmatrix} \text{ and } \mathbf{Q_{temp}} = \gamma\, \Sigma_{\mathbf{temp}},$$

γ being computed so that $\mathbf{Q_{temp}}(\mathrm{El} = 90^\circ) = 1$ (cofactor matrix).

Figure 7a shows an example of the structure of such a covariance matrix and Fig. 7b the corresponding skyplot. The smoothness parameter were taken to $\nu = 5/6$ and the inverse of the Mátern correlation time is $\alpha = 0.006\,\mathrm{s}^{-1}$.

Figure 7a highlights that the fully populated covariance matrices have a block diagonal structure; each sub matrices showing globally a "Toeplitz" like form. This property could be used in future to accelerate the inversion algorithm (Meurant 1992). The computation of such fully populated covariance matrices—one per batch—took only a few second for the whole observation time and is faster than the Schön and Brunner or Treuhaft and Lany model as no integration must be performed.

4.4 Results

In the following plots, black stars correspond to results with $\mathbf{Q}_\varepsilon$ called the EPS model, whereas blue or green circles are obtained with the fully populated cofactor matrices $\mathbf{Q}$ called CORR.

4.4.1 Baseline P0P1 of 1,000 m

Varying the smoothness factor

Figure 8 shows the ratio R_i (b) as well as the quadratic deviation (a) of the batch coordinates when changing the value of the smoothness parameter ν from 1/6 to 3/2 by keeping α constant, $\alpha = 0.006\,\mathrm{s}^{-1}$. This value corresponds to a physical relevant Mátern correlation time by taking $L_0 = 6000\mathrm{m}$ and $u = 8{-}10\,\mathrm{ms}^{-1}$ (see also Schön and Brunner 2008a). We plotted the results for two different values of the noise factor: $\beta = 0.3$ (blue circle) and $\beta = 0$ (green circle, no observation noise). Since the EPS model (black stars) does not depend on the smoothness factor, the results are not varying with ν and are only plotted for an easier visual comparison.

For the CORR model, the ratio R_i is close to 1 for nearly all values of ν by taking $\beta = 0.3$. The case $\beta = 0$ gives a ratio $R_i >> 1$. As expected, the EPS model is showing an overestimation of the precision, i.e. the standard deviation is smaller than the coordinate scatter.

With a noise factor $\beta = 0.3$ and for the value of interest $\nu = 5/6$, the Up and East component have a smaller quadratic deviation with the CORR model (but only at the sub-millimeter level), whereas the N component deviation giving a not significantly higher than the EPS model

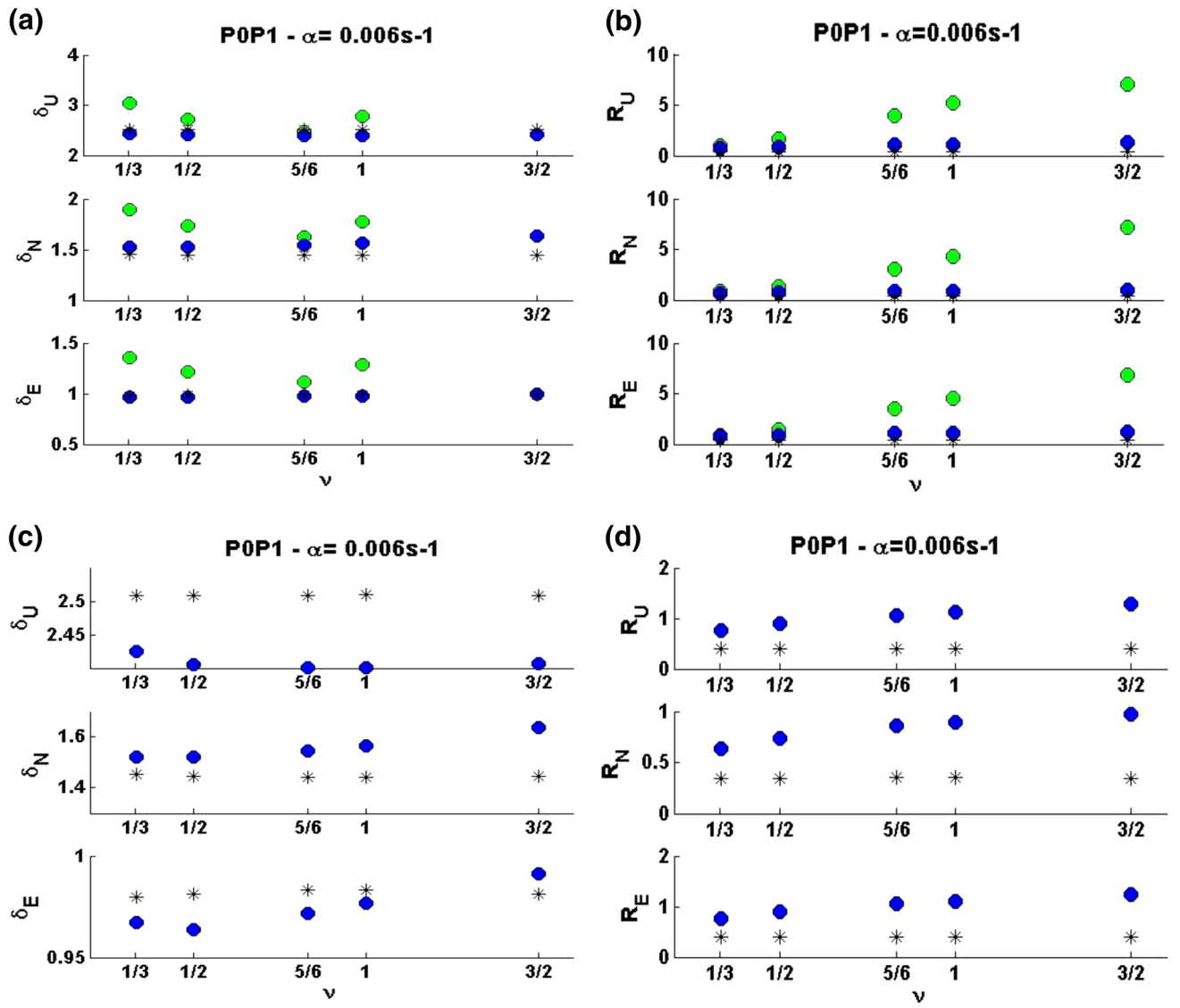

Fig. 8 Mean coordinate scatter δ_i (**a**) and ratio R_i (**b**) of the batch solutions are plotted for the N, E and U component versus smoothness factor ν for $\alpha = 0.006s^{-1}$. The values $\delta_i(\nu = 3/2)$ are higher than the other cases and not plotted for more readability. *Green circles* represent the CORR model with $\beta = 0$, *blue circles* $\beta = 0.3$ and *stars* the EPS model. **c** Zoom of **a**. **d** Zoom of **b**. Short baseline P0P1 (1,000 m)

(1.45 mm with EPS or 1.5 mm with CORR for $\nu = 5/6$). Higher values of the noise factor will lead to coordinate scatters that are comparable with the EPS model. The value of $\beta = 0.3$ gives the lowest quadratic deviation together with ratios of 1, which is coherent with the definition $\beta = \frac{\text{nugget}}{\text{sill}}$ of the structure function of the double differenced observations for the Seewinkel Network.

We can note moreover that the model with $\nu = 5/6$ is nearly equivalently performing than $\nu = 1/2$ (exponential model); $\nu = 1$ (AR(1) model) giving a lightly and not significant higher standard deviation for the E and N component. However, it should be noticed that the exponential model is giving a ratio R_i smaller than 1 for a comparable quadratic deviation, provided that the correlation length is taken accordingly. Thus, we should prefer the turbulence value of the smoothness parameter $\nu = 5/6$ which seems more reliable. Moreover, the physical interpretation is easier and allows an accurate estimation of the correlation time.

Varying the correlation time

In Fig. 9a, b, we varied the parameter $\alpha = \frac{\kappa_0 u}{a}$ for $\nu = 5/6$. It can be seen that value in the range $[6e^{-3}, 1e^{-2}]\,s^{-1}$ are giving ratio close to 1 for $\beta = 0.3$ as well as a lower quadratic deviation compared to the EPS model and the CORR model with $\beta = 0$. High values of α, i.e. small temporal correlations are leading asymptotically to the same result as the EPS model.

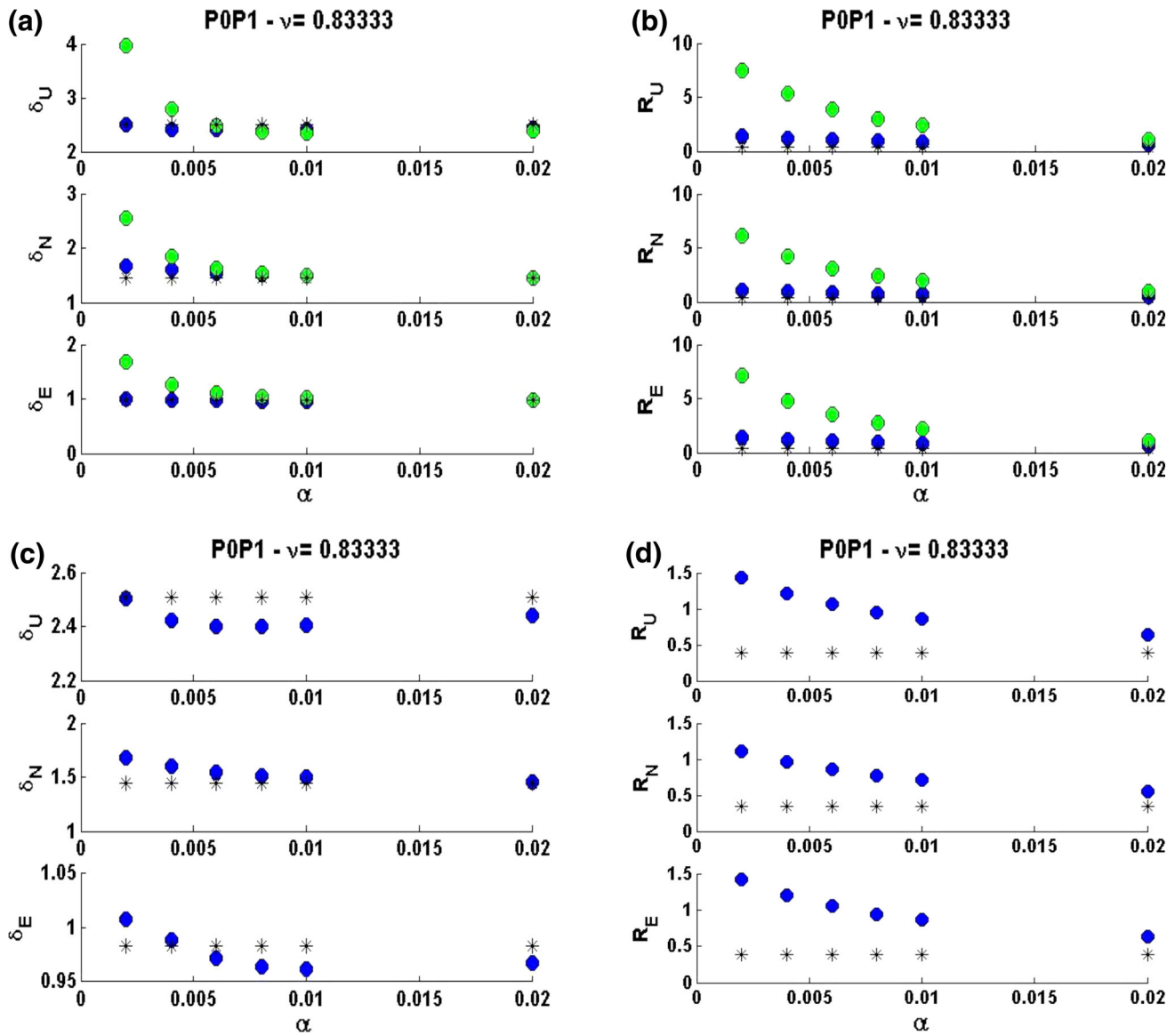

Fig. 9 Mean coordinate scatter δ_i (**a**) and ratio R_i (**b**) of the batch solutions are plotted for the N, E and U component versus α for $\nu = 5/6$. The values $\delta_i(\nu = 3/2)$ are higher than the other cases and not plotted for more readability. *Green circles* represent the CORR model with $\beta = 0$, *blue circles* $\beta = 0.3$ and *stars* the EPS model. **c** Zoom of **a**. **d** Zoom of **b**. Short baseline P0P1 (1,000 m)

From the study of the least-squares results (R_i and δ_i) for the baseline length 1,000 m, the values of $\nu = 5/6$ and $\alpha = 0,006\text{s}^{-1}$ seems to give accurate and relevant results. These values are coherent with values found by El-Rabbany (1994), Radovanovic (2001) or more recently Jansson and Persson (2013). It should be highlighted however that the differences between the different models are not very important as long as the Mátern parameters are taken in a reasonable interval.

1 s data rate

The results for the short baseline P0P1 at high data rate (1 s) were also estimated with 45 batches à 600 epochs. As before, the values of the smoothness parameters were changed as well as the value of the correlation time. It was found that the ratio R_i is close to 1 for $\nu = 5/6$. However, in this case, the noise factor was taken to 0.5, a slightly higher value as for the 30 s data rate. The coordinate scatter δ_i is smaller than those obtained with the EPS model, particularly for the Up and East components, although only in the sub-millimeter range. Once more, it was shown that varying the smoothness parameter in a reasonable range does not influence the results significantly.

The conclusions are the same as for the 30s rate: taking temporal correlations into account principally influence the

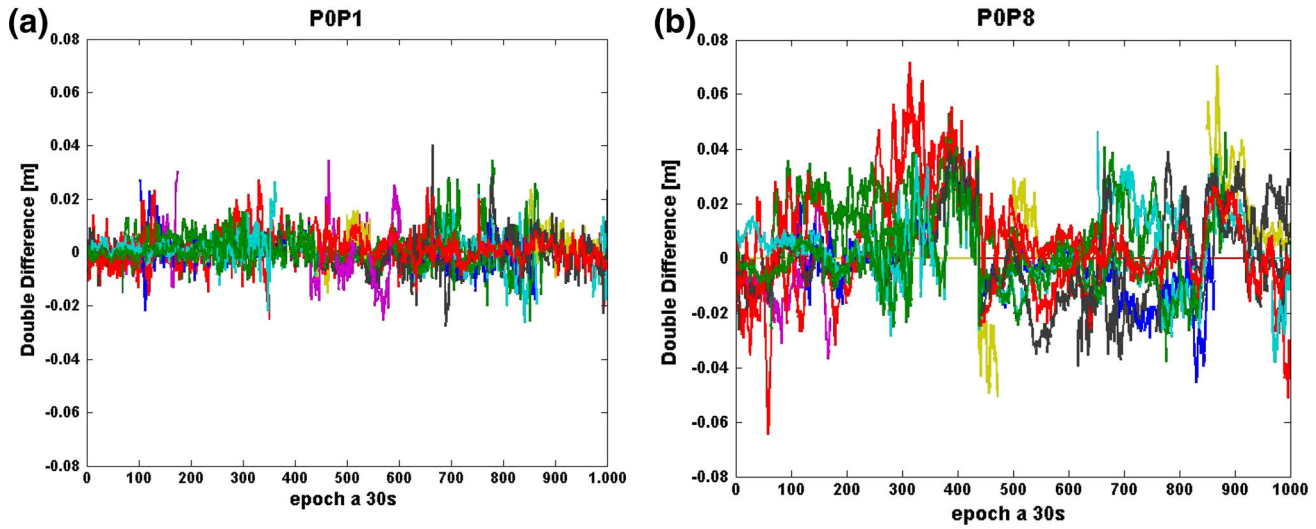

Fig. 10 Mean coordinate scatter δ_i (**a**) and ratio R_i (**b**) of the batch solution are plotted for the N, E and U component versus α for $\nu = 5/6$. *Green circles* represent the $CORR$ model with $\beta = 0.05$, *blue circles* $\beta = 0.3$ and *stars* the EPS model. Long baseline P0P8 (8,000 m)

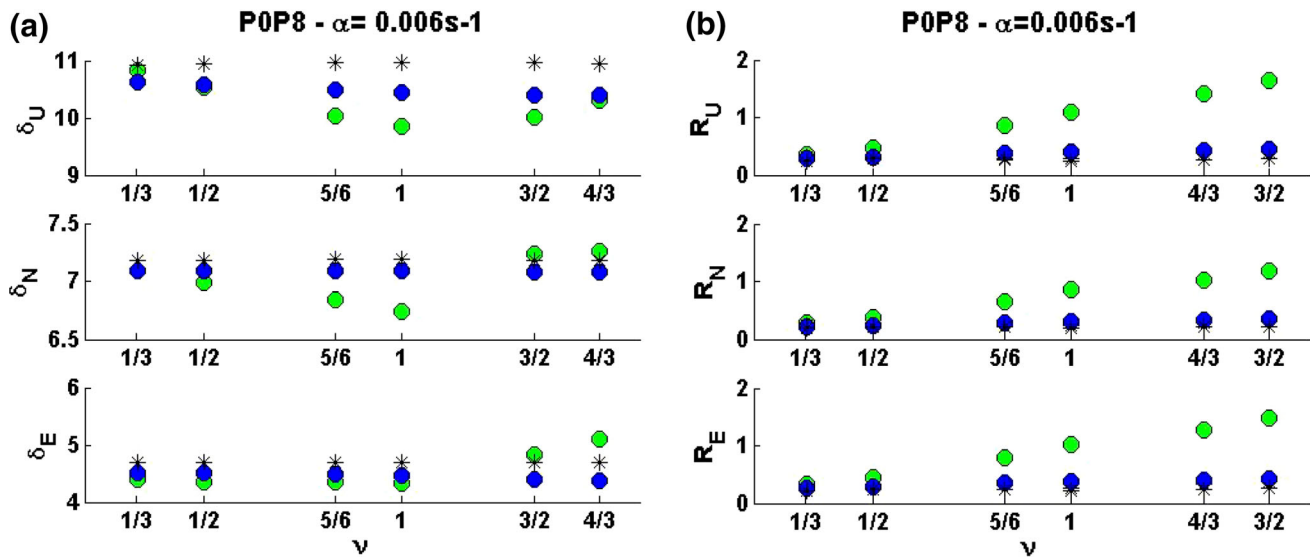

Fig. 11 Mean coordinate scatter δ_i (**a**) and ratio R_i (**b**) of the batch solution are plotted for the N, E and U component versus ν for $\alpha = 0.006s^{-1}$. *Green circles* represent the CORR model with $\beta = 0.05$, *blue circles* $\beta = 0.3$ and stars the EPS model. Long baseline P0P8 (8,000 m)

a posteriori variance. The spatial repartition of the parameter deviation (scatter) is not changing much as long as the Mátern parameters are not too far from 1. However, the a posteriori precision is more relevant and more accurate than with elevation-dependent diagonal covariance matrices.

4.4.2 Baseline P0P8 of 8,000 m

The same analysis was performed for the baseline P0P8 (8,000 m) with the same methodology. For a long baseline, other noise processes interact and the correlations are not only due to tropospheric fluctuations. Thus, in this part, we aim to show the impact of changing the Mátern covariance parameters α, ν on the least-squares adjustments. The results are presented in Figs. 11 and 10. As for the previous baseline P0P1, the value of the smoothness parameter (Fig. 11) $\nu = 5/6$ gives good results in term of ratio R_i and quadratic deviation δ_i which is smaller than with the EPS model. It should be mentioned that the noise factor of 0.05 gives the best results and not $\beta = 0.3$ as previously for the short baseline. It would mean that the nugget effect is close to 0, thus the cofactor of the observation noise is much smaller than for the short baseline of the Seewinkel Network.

The value of $\nu = 1$ provides lower values of δ_i, however with a light underestimation of the precision since $R_i > 1$. This is in agreement with the intuitive results that double

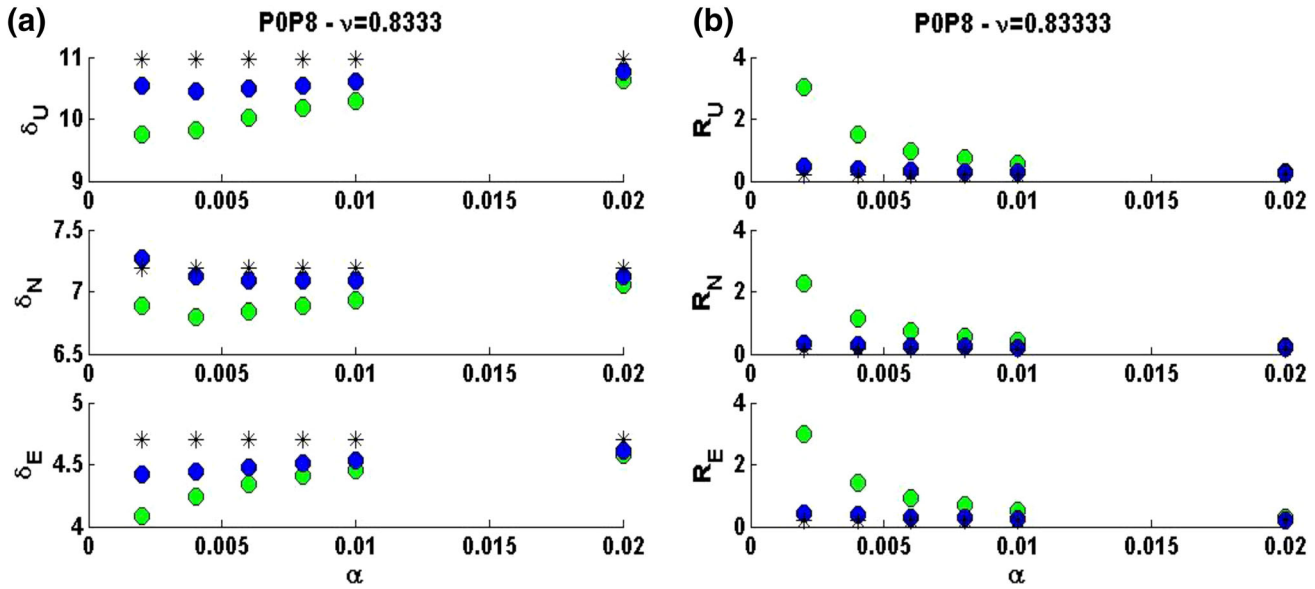

Fig. 12 **a** 8 h (30,000 s) of double differences for the 1,000 m baseline P0P1 and **b** 8 h (30,000 s) double differences for the 8,000 m baseline P0P8. Each satellite pair is color coded, the sampling rate is 30 s

differences from long baseline (Fig. 12b) are less smooth (Fig. 12a) than for shorter baseline since not all effects are canceled by double differencing, like, i.g. ionospheric propagation effects. This difference in term of standard deviation is however not very important (sub-millimeter level) and should be carefully interpreted by analyzing at the same time the values of R_i. This effect will be studied in the future for longer baselines.

Figure 10 presents the results of the least-squares adjustment when α is varied. As for the variation of the smoothness factor, β should be set close to 0. The value of $\alpha = 0.006\,\mathrm{s}^{-1}$ gives at the same time an improved coordinate scatter compared with the EPS model as well as a ratio of 1 for all three components. Smaller values of α $(0.002-0.004\,\mathrm{s}^{-1})$ gives also small values of δ_i, however, as with higher values of ν, with $R_i >> 1$.

The improvement of the CORR model with $\beta = 0.05$, $\nu = 5/6$, $\alpha = 0.006\ \mathrm{s}^{-1}$ is at the millimeter level for all three components in comparison with the EPS model, the ratio being at the same time more than 3 times better than with the standard model which remains a great improvement.

5 Conclusion

Temporal correlations of GNSS phase measurements due to tropospheric fluctuations are not taken in consideration in the currently used weighted least-squares models. The result is an overestimation of the a posteriori precision by up to a factor 10. Results of the Kolmogorov turbulence theory were used to develop a new and simplified model for the temporal correlations thanks to the Mátern covariance family which best suits to model both the temporal correlations for one satellite and for two satellites observed at one or two separated stations. The concepts of separation distance as well as inhomogeneity and anisotropy were taken in consideration. Using Taylor's frozen hypothesis, it was shown that a smoothness parameter of 5/6 as well as a Mátern correlation time between 125 and 200 s, in accordance with previous studies, should correctly model temporal correlations due to the tropospheric propagation. Moreover, it was stressed that all other parameters such as the structure constant, the depth or height of the troposphere as well as the vertical elongated parameter or the outer scale length should be carefully chosen.

In a case study, we used the data of the Seewinkel Network, specially designed for research on the effect of tropospheric fluctuations on GPS phase measurements, with weak multipath. Fully populated cofactor matrices were computed and compared with diagonal matrices of type $\frac{1}{\sin^2(\mathrm{El})}$ which are widely used in current processing softwares. To model other noise effects, an elevation-dependent diagonal matrix was added to the temporal cofactor matrices. It was shown that for the short baseline, fully populated cofactor matrices improves the quadratic deviation of the coordinates at the sub-millimeter level for short baseline and at the millimeter level for long baseline) compared with elevation dependant models. However, the a posteriori precision is more reliable than with diagonal matrices, i.e. no overestimation occurs. The results were similar for longer baseline (8,000 m) as well as for higher data rate (1 s), although for long baseline a higher smoothness factor than 5/6 could be taken in con-

sideration. The new model leads globally to a slightly better and physically more relevant results in terms of quadratic deviation of the coordinates and a posteriori variance of the unknowns than the exponential and AR(1) model. Thus the proposed formula with a smoothness factor of $\nu = 5/6$ is promising, particularly for short baselines. As no double integrations are performed such as in other models (Treuhaft and Lany, Schön and Brunner) the computational time remains manageable. Some simplifications due to the Toeplitz like form of the covariance matrices could moreover lead to a faster implementation.

Modeling temporal correlations with the turbulence theory and Mátern cofactor function has lead to improved results in the least-squares solution, being at the same time technically feasible. In a next work, the impact on ambiguity resolutions will be shown as well as the influence of outliers on the parameters. Depending on the baseline length the choosing of the Mátern parameters could be moreover studied by minimum likelihood estimation.

Acknowledgments The authors gratefully acknowledge the funding by the DFG under the label SCHO1314/1-2. Fritz K. Brunner is warmly thanked for discussions on turbulence theory and for providing the GPS data of the Seewinkel Network. The valuable comments of three anonymous reviewers helped us improve significantly the manuscript.

Appendix: The Mátern covariance functions

A short introduction to the Mátern covariance family, also called Whittle Mátern covariance family, von Karman model (oceanography), Markov processes (geodesy) or autoregressive models (meteorology) is presented here, giving the principal features, vocabulary as well as dependencies. More details can be exemplarily found in Stein (1999), Mátern (1960), Guttorp and Gneiting (2005), Grafarend and Awange (2012). Mátern covariance functions have been concretely used by Handcock and Wallis (1994) to model meteorological fields. Fuentes (2002) also derived a non stationary family for the determination of air quality models.

A 2D autoregressive continuous process AR(1) called $Z(x, y)$ can be described by the stochastic differential equation:

$$\left(\frac{\partial}{\partial x^2}^2 + \frac{\partial}{\partial y^2}^2 - \alpha^2\right) Z(x, y) = \varepsilon(x, y), \tag{21}$$

where $\varepsilon(x, y)$ is white noise and α a constant. The corresponding spectral density is given by

$$W(\omega) \propto \frac{1}{(\omega^2 + \alpha^2)^2}, \tag{22}$$

with $\omega^2 = \omega_1^2 + \omega_2^2$ for the 2D case (Whittle 1954). The stationary covariance between two points $\mathbf{x}, \mathbf{x}'$ for this process is:

$$C(\mathbf{x}, \mathbf{x}') = C(r) = (\alpha r) K_1(\alpha r), \tag{23}$$

where K_1 is the modified Bessel function of 1st order, $r = \|\mathbf{x} - \mathbf{x}'\|$ for the isotropic case ($\|.\|$ being the norm of the vector). Whittle (1954) presented such a covariance function as a "natural spatial covariance" for the 2D case, as the exponential-based covariance functions are for one-dimensional processes.

Mátern (1960) used Whittle's result and derived for any dimension d a family of covariance functions based on an isotropic spectral density:

$$W(\omega) = \frac{2^{\nu-1}\phi \quad \Gamma(\nu + d/2)\,\alpha^{2\nu}}{\pi^{d/2}(\omega^2 + \alpha^2)^{\nu+d/2}}, \tag{24}$$

where $\omega^2 = \omega_1^2 + \omega_2^2 + ... + \omega_d^2$ is the angular frequency, Γ the Gamma function (Abramowitz and Segun 1972) and $\nu > 0, \alpha > 0, \phi > 0$ are constant parameters, d the dimension. The corresponding Mátern class of covariance functions is positive definite and reads:

$$C(r) = \phi (\alpha r)^{\nu} K_{\nu}(\alpha r). \tag{25}$$

The parameter ν can be seen as a measure of the differentiability of the field (Stein 1999) thus "its smoothness". The constant α indicates how the correlations decay with increasing distance. Its inverse is usually called the correlation length in Kriging.

Smoothness parameter ν

Figure 13 highlights the influence of the smoothness parameter ν and the correlation length by simulating a random field/time series corresponding to the covariance function (Cressie 1993) using the eigenvalue decomposition of the corresponding Toeplitz covariance matrix (Vennebusch et al. 2010). The same random vector was used for each simulation.

The smoothness parameter ν was varied from 1/6 to 3. As ν increases, the time series are becoming less noisy for high frequency, the long periodic variations are predominating. The variance is decreasing with the smoothness parameter.

Correlation time

Figure 14 shows the influence of the parameter α. It was varied from 0.25 to 1 by keeping ν constant to 1 to simulate short and long correlation times.

Using the previous parametrization of the Mátern covariance family, the variance is not varying with the correlation time. The simulations of time series (Fig. 14b) highlight that changes of the correlation time are not acting on the smoothness of the field.

Other parametrizations

In the literature, further formulation of these covariance family functions are given (Handcock and Wallis 1994) where the parameter ρ, $\rho > 0$ is nearly independent of ν:

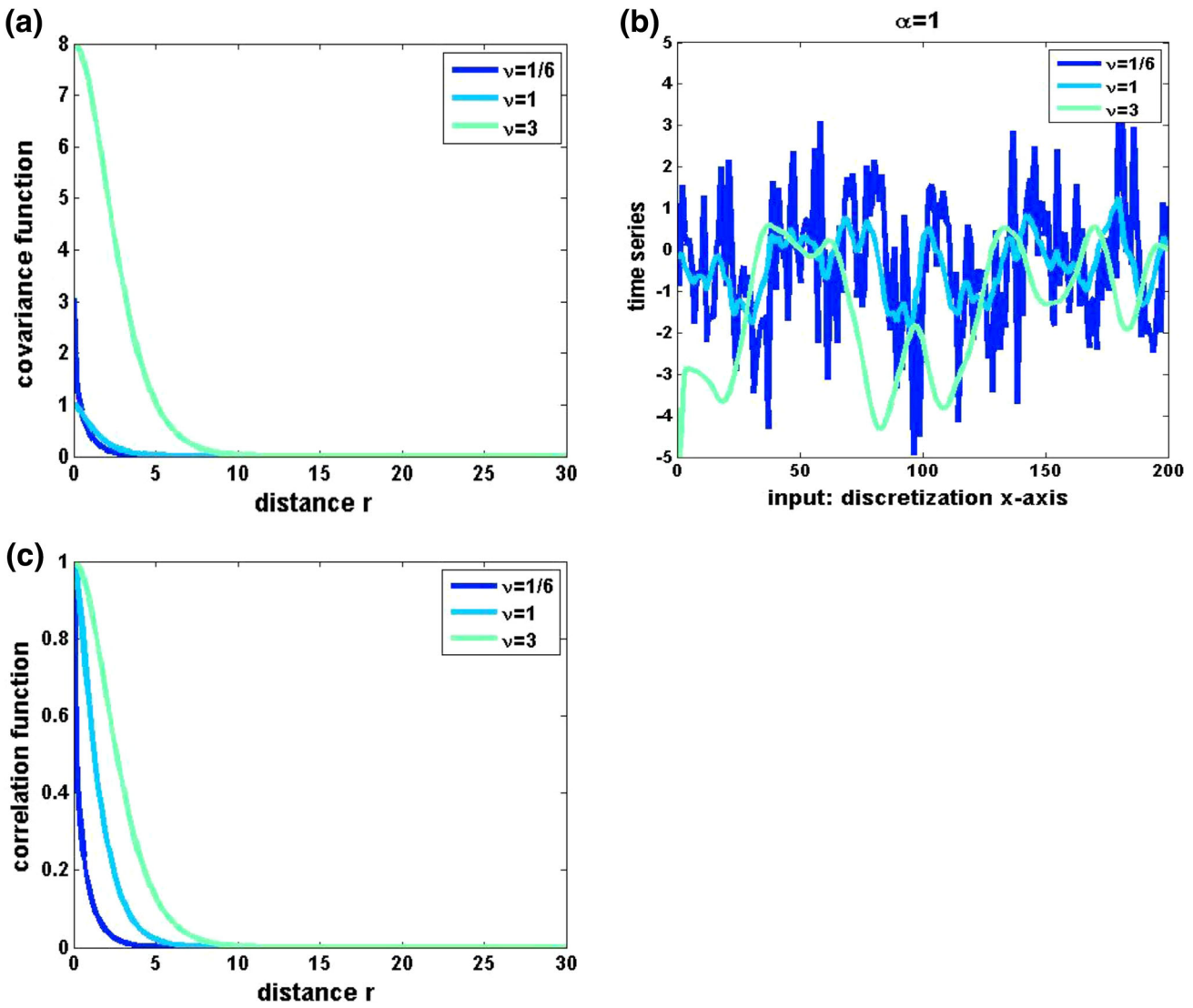

Fig. 13 **a** Covariance function (Màtern family) with $\alpha = 1$ by varying ν and **b** corresponding time series. The x axis was discretized of 200 equally spaced points. **c** Corresponding correlation function

$$C(r) = \frac{2^{1-\nu}}{\Gamma(\nu)} \left(\frac{\sqrt{2\nu} r}{\rho} \right)^{\nu} K_{\nu} \left(\frac{\sqrt{2\nu} r}{\rho} \right),$$

with a spectral density of the form:

$$W(\omega) = \frac{2^d \pi^{d/2} \Gamma(\nu + d/2) (2\nu)^{\nu}}{\Gamma(\nu) \rho^{2\nu}} \left(\frac{2\nu}{\rho^2} + \omega^2 \right)^{-(\nu + d/2)}.$$

This parametrization is said to be more stable when estimating the parameters ν, α with the maximum likelihood method (Stein 1999). We made use of it to develop our model for GPS phase correlations.

Shkarofsky (1968) presented a more general form of the Mátern model by introducing a shape parameter $\delta > 0$. The corresponding correlation function reads:

$$C(r) = \frac{1}{\delta^{\nu} K_{\nu}(\delta)} \left(\frac{r^2}{L^2} + \delta^2 \right)^{\nu/2} K_{\nu} \left(\sqrt{\frac{r^2}{L^2} + \delta^2} \right).$$

Thus with $\delta = 0$, the Mátern family is obtained.

If is half-integer, the covariance can be expressed in term of a product of an exponential and a polynomial of order p (Rasmussen and Williams 2006): for $\nu = 1/2$, the exponential model is obtained whereas for $\nu = 3/2, C(r) = \left(1 + \frac{\sqrt{3}r}{\rho}\right) \mathrm{e}^{-\frac{\sqrt{3}r}{\rho}}$, which corresponds to a Markov process of second order and for $\nu = 5/2$, a Markov process of third order.

Advantage of the Mátern family

The advantages of the Mátern covariance functions' family for spatial interpolation are multiple, as developed in Stein (1999). Its flexibility to model the smoothness of physical processes (thus the rate of decay of the spectral density at high frequencies) is particularly useful, as well as the possibility to include non-stationarity or anisotropy (Fuentes 2002; Spöck

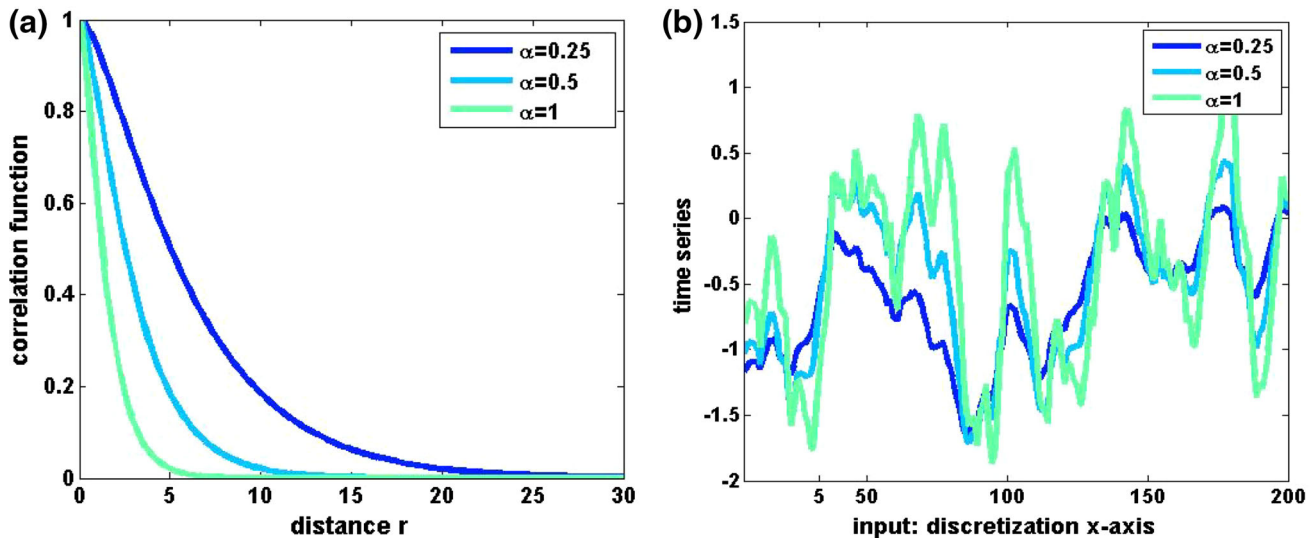

Fig. 14 **a** Covariance function (Mátern family) with $\nu = 1$ by varying α and **b** the corresponding time series. The x axis was discretized of 200 equally spaced points

and Pilz 2008). The degree of smoothness can be estimated a priori or being fixed in advance and the number of parameters to manage stays reasonable. The exponential ($\nu = \frac{1}{2}$) and Gaussian case ($\nu = \infty$) are two particular cases of this family although the last one that represents an infinitely differentiable field is concretely rarely found (Stein 1999; Handcock and Wallis 1994).

References

Abramowitz M, Segun IA (1972) Handbook of mathematical functions. Dover, New York edition

Beutler G, Bauersima I, Gurtner W, Rothacher M (1987) Correlations between simultaneous GPS double difference carrier phase observations in the multistation mode: Implementation considerations and first experiences. Manusc. Geod. 12(1):40–44

Böhm J, Schuh H (2013) Atmospheric effects in space geodesy. Springer, Berlin

Borre K, Tiberius C (2000) Time series analysis of GPS observables. In: Proceedings of ION GPS 2000, Salt Lake City, UT, USA, September 19–22, pp 1885–1894

Brunner FK, Hartinger H, Troyer L (1999) GPS signal diffraction modelling: the stochastic SIGMA-δ model. J Geod 73(5):259–267

Coulman CE, Vernin J (1991) Significance of anisotropy and the outer scale of turbulence for optical and radio seeing. Appl Opt 30(1):118–126

Cressie N (1993) Statistics for spatial data. Wiley, New York

Dach R, Brockmann E, Schaer S, Beutler G, Meindl M, Prange L, Bock H, Jäggi A, Ostini L (2009) GNSS processing at CODE: status report. J Geod 83(3–4):353–365

El-Rabbany A (1994) The effect of physical correlations on the ambiguity resolution and accuracy estimation in GPS differential positioning. PhD thesis, Department of Geodesy and Geomatics Engineering, University of New Brunswick, Canada

Euler HJ, Goad CC (1991) On optimal filtering of GPS dual frequency observations without using orbit information. Bull Géodésique 65(2):130–143

Farge M (1992) Wavelet transform and their applications to turbulence. Ann Rev Fluid Mech 24:395–457

Fuentes M (2002) Spectral methods for nonstationary processes. Biometrika 89:197–210

Gage KS (1979) Evidence for a k to the -5/3 law inertial range in mesoscale two-dimensional turbulence. J Atmos Sci 36:1950–1954

Gradinarsky LP (2002) Sensing atmospheric water vapor using radio waves. Ph.D. thesis, School of Electrical Engineering, Chalmers University of Technology, Göteborg, Sweden

Grafarend EW (1976) Geodetic applications of stochastic processes. Phys Earth Planet Inter 12(2–3):151–179

Grafarend EW, Awange J (2012) Applications of linear and nonlinear models. Springer, Berlin

Guttorp P, Gneiting T (2005) On the Whittle–Mátern correlation family. NRCSE technical report series n°80

Handcock MS, Wallis JR (1994) An approach to statistical spatial–temporal modeling of meteorological fields. J Am Stat Assoc 89(426):368–378

Hartinger H, Brunner FK (1999) Variances of GPS phase observations: the SIGMA-ε model. GPS Sol 2(4):35–43

Howind J, Kutterer H, Heck B (1999) Impact of temporal correlations on GPS-derived relative point positions. J Geod 73(5):246–258

Hunt JCR, Morrison JF (2000) Eddy structure in turbulent boundary layers. Eur J Mech B Fluids 19:673–694

Ishimaru A (1997) Wave propagation and scattering in random media. IEEE Press and Oxford University Press, New York

Jansson P, Persson CG (2013) The effect of correlation on uncertainty estimates—with GPS examples. J Geod Sci 3(2):111–120

Jones RH, Vecchia AV (1993) Fitting continuous ARMA models to unequally spaced spatial data. J Am Stat Assoc 88(423):947–954

Khujadze G, Nguyen van yen R, Schneider K, Oberlack M, Farge M (2013) Coherent vorticity extraction in turbulent boundary layers using orthogonal wavelets . J. Phys. Conf. Ser. 318:022011

Kleijer F (2004) Tropospheric modeling and filtering for precise GPS leveling. PhD Thesis Netherlands Geodetic Commission, Publications on Geodesy 56

Kolmogorov NA (1941) Dissipation of energy in the locally isotropic turbulence. Proc USSR Acad Sci 32:16–18 (Russian)

Kraichnan RH (1974) On Kolmogorov's inertial range theories. J Fluid Mech 62(2):305–330

Kutterer H (1999) On the sensitivity of the results of least-squares adjustments concerning the stochastic model. J Geod 73:350–361
Lesieur M (2008) Turbul Fluids, 4th edn. Springer, The Netherlands
Luo X, Mayer M, Heck B (2012) Analysing time series of GNSS residuals by means of ARIMA processes. Int Assoc Geod Symp 137:129–134
Luo X, Mayer M, Heck B (2011) A realistic and easy-to-implement weighting model for GNSS phase observations. In: International union of geodesy and geophysics (IUGG), General Assembly 2011 - Earth on the Edge: Science for a Sustainable Plane, Melbourne, Australia, 28.06.-07.07.2011
Mátern B (1960) Spatial variation-stochastic models and their application to some problems in forest surveys and other sampling investigation. Medd. Statens Skogsforskningsinstitut 49(5)
Meurant G (1992) A review on the inverse of tridiagonal and block tridiagonal matrices. SIAM J Matrix Anal Appl 13(3):707–728
Monin AS, Yaglom AM (1975) Statistical fluid mechanics, vol 2. MIT Press, Cambridge
Nilsson T, Haas R (2010) Impact of atmospheric turbulence on geodetic very long baseline interferometry. J Geophys Res 115:B03407
Pany A, Böhm J, MacMillan D, Schuh H, Nilsson T, Wresnik J (2011) Monte Carlo simulations of the impact of troposphere, clock and measurement errors on the repeatability of VLBI positions. J Geod 85:39–50
Radovanovic RS (2001) Variance–covariance modeling of carrier phase errors for rigorous adjustment of local area networks, IAG 2001 Scientific Assembly. Budapest, Hungary, September 2–7, 2001
Rao C, Toutenburg H (1999) Linear models. Least-squares and alternatives, 2nd edn. Springer, New York
Rasmussen CE, Williams C (2006) Gaussian processes for machine learning. The MIT Press, New York
Romero-Wolf A, Jacobs CS, Ratcli JT (2012) Effects of tropospheric spatio-temporal correlated noise on the analysis of space geodetic data. In: IVS general meeting proceedings, Madrid, Spain, March 5–8, 2012
Satirapod C, Wang J, Rizos C (2003) Comparing different GPS data processing techniques for modelling residual systematic errors. J Surv Eng 129(4):129–135
Schön S, Kutterer H (2006) A comparative analysis of uncertainty modeling in GPS data analysis. In: Rizos C, Tregoning P (eds) Dynamic planet - monitoring and understanding a dynamic planet with geodetic and oceanographic tools. International Association of Geodesy Symposia, vol 130. Springer, Berlin, Heidelberg, New York pp 137–142
Schön S, Brunner FK (2007) Treatment of refractivity fluctuations by fully populated variance-covariance matrices. In: Proc. 1st colloquium scientific and fundamental aspects of the Galileo programme Toulouse Okt
Schön S, Brunner FK (2008a) Atmospheric turbulence theory applied to GPS carrier-phase data. J Geod 1:47–57
Schön S, Brunner FK (2008b) A proposal for modeling physical correlations of GPS phase observations. J Geod 82(10):601–612
Shrakrofsky IP (1968) Generalized turbulence space-correlation and wave-number spectrum-function pairs. Can J Phys 46:2133–2153
Spöck G, Pilz J (2008) Non-spatial modeling using harmonic analysis. VIII Int. Geostatistics congress, Santiago, 2008, pp 1–10
Stein ML (1999) Interpolation of spatial data. Some theory for kriging. Springer, New York
Stull RB (2009) An introduction to boundary layer meteorology. Springer, Berlin
Tatarskii VI (1971) Wave propagation in a turbulent medium. McGraw-Hill, New York
Taylor GI (1938) The spectrum of turbulence. In: Proceedings of the Royal Society London, Seires A CLXIV, pp 476–490
Treuhaft RN, Lanyi GE (1987) The effect of the dynamic wet troposphere on radio interferometric measurements. Radio Sci 22(2):251–265
Tikhonov AN, Goncharsky AV, Stepanov VV, Yagola AG (1995) Numerical methods for the solution of Ill-posed problems. Kluwer Academic Publishers, Dordrecht
Vennebusch M, Schön S, Weinbach U (2010) Temporal and spatial stochastic behavior of high-frequency slant tropospheric delays from simulations and real GPS data. Adv Space Res 47(10):1681–1690
Voitsekhovich VV (1995) Outer scale of turbulence: comparison of different models. J Opt Soc Am A 12(6):1346–1353
Wang J, Satirapod C, Rizos C (2002) Stochastic assessment of GPS carrier phase measurements for precise static relative positioning. J Geod 76(2):95–104
Wheelon AD (2001) Electromagnetic scintillation part I geometrical optics. Cambridge University Press, Cambridge
Whittle P (1954) On stationary processes in the plane. Biometrika 41(434):449
Wieser A, Brunner FK (2000) An extended weight model for GPS phase observations. Earth Planet Space 52:777–782
Williams S, Bock Y, Fang P, Jamason P, Nikolaidis RM, Prawirodirdjo L, Miller M, Johnson DJ (2004) Error analysis of continuous GPS position time series. J Geophys Res 109:B03412